Assignment of the Axial Ligands of Ferric Ion in Low-Spin Hemoproteins by Near-Infrared Magnetic Circular Dichroism and Electron Paramagnetic Resonance Spectroscopy

Paul M. A. Gadsby and Andrew J. Thomson*

Contribution from the School of Chemical Sciences, University of East Anglia, Norwich NR4 7TJ, U.K. *Received May 22, 1989*

Abstract: The energies (E_{CT}) of the porphyrin (π) to ferric (t_{2g}) ion charge-transfer (CT) transitions of 34 low-spin ferric hemoproteins have been determined by near-infrared magnetic circular dichroism (MCD) spectroscopy at 4.2 K and 5 T. The proteins all have protoheme IX with histidine as the proximal ligand and a variety of second axial ligands. The EPR g values of the same derivatives have been measured, enabling the low-symmetry axial (Δ) and rhombic (V) crystal field parameters to be calculated. It is shown that there is a positive empirical correlation between E_{CT} and E_{yz} ($=\Delta/3 + V/2$ in units of Fe spin-orbit coupling), the energy of the Fe(III) hole relative to the baricenter of the t_{2g} 3d subshell. This correlation provides a protocol for axial ligand assignment of low-spin ferric protoheme IX in proteins. Six different axial ligation states that may arise by use of an amino acid side chain are considered. They are methionine-histidine (E_{CT} 1740-1950 nm), histidine-histidine or histidine-imidazole (which is taken to be the equivalent) (E_{CT} 1500-1630 nm), histidine-histidinate (or imidazolate) (E_{CT} 1350-1370 nm), methionine-histidinate (E_{CT} 1550 nm), lysine-histidine (E_{CT} 1480-1550 nm), and thiolate-histidine (E_{CT} 1035-1200 nm). Where discrimination on the basis of E_{CT} alone is impossible, additional spectral evidence is needed. The protocol proposed requires measurement of *both* EPR and near-IR MCD spectra. This is especially necessary to identify ligation by histidinate, when lysine-histidine ligation is suspected or when the heme is subject to a crystal field of low rhombicity and high axiality. The last two cases give rise to EPR spectra with high g_{max} values, with a Gaussian line shape in the case of lysine-histidine, and with a folded shape for bis(histidine) ligation. In neither case can the g_x and g_y values be observed. Finally, the near-IR MCD spectra of the cyanide adducts can be used to identify the nature of the proximal ligand.

1. Introduction

The assignment of axial ligands of the heme iron in hemoproteins by spectroscopic methods provides an adjunct to the evidence from crystallography and enables relationships between function and structural variation to be charted. This is important in the case of complex multicentered heme proteins. For proteins containing low-spin ferric protoheme IX, electron paramagnetic resonance (EPR) spectroscopy has been a widely used technique for axial ligand assignment.[1] A large number of proteins have been studied and the results calibrated with hemoproteins of well-defined structure.[2] The spectra are characterized by an anisotropic rhombic **g** tensor invariably with two principal values above the free electron value and one below.[3] The analysis of the spectra, first given by Griffiths,[4] is readily made in terms of a distorted octahedral, low-spin (t_{2g})^5 complex. The ground state of this configuration is a Kramers doublet arising from a positive hole occupying the $d_{xy,yz,xz}$ orbitals, which are subject to low-symmetry crystal field distortions, axial (Δ) and rhombic (V), and to spin-orbit coupling (λ). Since the latter parameter varies very little between hemoproteins, the two crystal field distortion parameters can be derived from the experimental EPR spectra.[3] A plot of the rhombic (V/λ) versus the tetragonal (Δ/λ) field for proteins containing heme iron shows that points for hemes of the same ligation state fall within clusters on the diagram.[1] However, this method has its shortcomings and uncertainties. For a given type of axial ligation there can be considerable variation in the EPR g values, as between different proteins. For example, coordination by two histidine ligands can give rise to low-spin hemoproteins with g_z values varying between 3.05, as in the case of cytochrome b_5 from liver,[5] and 3.5, in the case of membrane-bound cytochrome b_{558} (*Bacillus subtilis*).[6] There is evidence from spectroscopic and crystallographic data on model compounds that the relative orientation of the two histidine ring planes and the orientation of the ring plane relative to the heme pyrrole nitrogen atoms can affect the g values, varying g_{max} between ~3.0 and ~3.6.[7] In cases where the g_z component of the **g** tensor is greater than ~3.4, the other two components g_x and g_y become difficult to detect experimentally.[8] In the absence of knowledge of the other components of the tensor it is not possible to establish unambiguously the crystal field parameters of the heme. Therefore, the EPR method of ligand assignment is inapplicable. Hence, for secure axial ligand assignment, it is desirable to apply a number of complementary methods.

The optical spectra of low-spin ferric hemoproteins provide another method of axial ligand assignment. It is now well established that there are transitions in the near-infrared (near-IR) region between 700 and 3000 nm, in addition to thee optical transitions arising from the porphyrin π electrons in the visible and near-UV regions.[9] These are charge-transfer (CT) transitions from the highest filled porphyrin orbitals, a_{1u} and $a_{2u}(\pi)$, to the positive hole in the t_{2g} subshell of the ferric d orbitals (Figure 1). Hence, the energies of these transitions depend upon the energy of the hole on the ferric ion relative to that of the filled porphyrin orbitals. It has been shown that the energy of this transition (E_{CT}) is markedly dependent upon the nature of the axial heme iron ligands.[9-16] However, the detection of the absorption band due

(1) Blumberg, W. E.; Peisach, J. In *Probes of Structure and Functions of Macromolecules and Membranes*; Chance, B., Yonetani, T., Mildvan, A. S., Ed.; Academic Press: New York, 1971; Vol. 2, pp 215-229.
(2) Brautigan, D. L.; Feinberg, B. A.; Hoffman, B. M.; Margoliash, E.; Peisach, J.; Blumberg, W. E. *J. Biol. Chem.* **1977**, *252*, 574-582.
(3) Taylor, C. P. S. *Biochim. Biophys. Acta* **1977**, *491*, 137-149.
(4) Griffith, J. S. *Nature (London)* **1957**, *180*, 30-31.
(5) Ikeda, M.; Iizuka, T.; Takao, H.; Hagihara, B. *Biochim. Biophys. Acta* **1974**, *336*, 15-24.
(6) Andersson, K. K.; Hederstedt, L. *J. Bacteriol.* **1986**, *167*, 635-639.
(7) Walker, F. A.; Huynh, B. H.; Scheidt, W. R.; Osvath, S. R. *J. Am. Chem. Soc.* **1986**, *108*, 5288-5297.
(8) Salerno, J. C. *J. Biol. Chem.* **1984**, *259*, 2331-2336.
(9) Smith, D. W.; Williams, R. J. P. *Struct. Bonding* **1970**, *7*, 1-45.
(10) Day, P.; Smith, D. W.; Williams, R. J. P. *Biochemistry* **1967**, *6*, 3747-3750.
(11) Cheng, J. C.; Osborne, G. A.; Stephens, P. J.; Eaton, W. A. *Nature (London)* **1973**, *241*, 193-194.
(12) Stephens, P. J.; Sutherland, J. C.; Cheng, J. C.; Eaton, W. A. In *Excited States of Biological Molecules*; Birks, J. B., Ed.; Wiley: New York, 1974; pp 434-442.
(13) Schejter, A.; Eaton, W. A. *Biochemistry* **1984**, *23*, 1081-1084.
(14) Rawlings, J.; Stephens, P. J.; Nafie, L. A.; Kamen, M. D. *Biochemistry* **1977**, *16*, 1725-1729.
(15) Nozawa, T.; Yamamoto, T.; Hatano, M. *Biochim. Biophys. Acta* **1976**, *427*, 28-37.

0002-7863/90/1512-5003$02.50/0

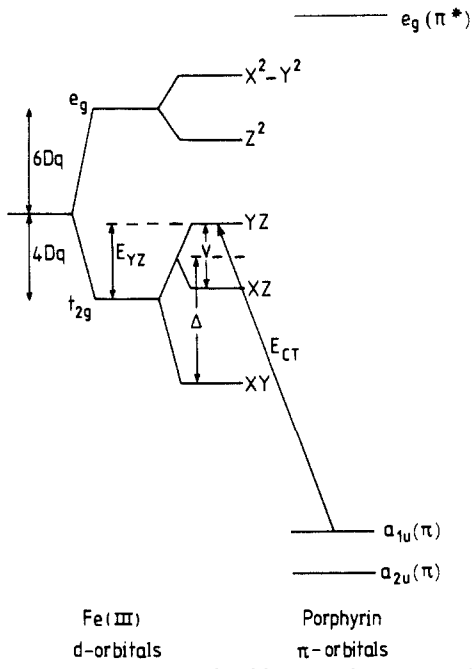

Figure 1. d-orbital energy levels of low-spin ferric ion and the π,π^* orbitals of the porphyrin ring showing the optical transitions predicted between the highest filled porphyrin π levels and the d orbitals. The definitions of E_{CT}, E_{yz}, Δ, and V are also indicated.

to this transition becomes increasingly difficult experimentally as its wavelength lies toward 2000 nm. This is because the spectral region is partially obscured by the vibrational overtone peaks arising from C–H, O–H, and N–H groups of the protein. Exchange of protons by deuterons causes the vibrational peaks to move to longer wavelength. However, not all protons in proteins are easily exchanged. This difficulty can be overcome by the measurement of the magnetic circular dichroism (MCD) spectra of hemoproteins in this wavelength range.[11] The intensity of the MCD spectrum depends, inter alia, upon the magnetic moments of the particle involved in the transition. Since the magnetic moments of nuclei are several orders of magnitude smaller than that of the electron, the MCD signals of vibrational transitions are several orders of magnitude weaker than those of electronic transitions.[17] By making measurements on samples held at very low temperatures, ~4.2 K, the intensity of the MCD spectrum of an electronic transition of a paramagnetic species is further increased compared with that of vibrational transitions. However, measurements can be made both at room temperature and at 4.2 K, enabling thermally induced spin state changes or ligand exchanges to be monitored. In addition, the MCD spectrum is a signed quantity with an absolute intensity that depends upon the symmetry of the crystal field at the ferric ion. This yields additional useful information.

We have been systematically collecting the near-IR MCD spectra at 4.2 K and room temperature of a range of hemoproteins in order to locate the porphyrin to ferric CT transitions.[18] In this paper the data are gathered together and analyzed. It is shown that for a variety of low-spin ferric hemoproteins there is a correlation between the energy of the positive hole on the ferric ion, as determined experimentally from the EPR g values, and the energy of the CT band as located by MCD spectroscopy. The examples all contain the protoheme IX ring with histidine as the proximal ligand and a further ligand bound in the second axial positions. The latter have a range of crystal field strengths covering much of the spectrochemical series although in every case the heme is low spin. This correlation puts the assignment of the near-IR CT bands of low-spin ferric hemoproteins on a more secure basis and provides a useful linear relationship between the energy of the hole and the CT band, which should have predictive value as well as assisting in the axial ligand assignment. During the course of this work Schejter and Eaton[13] also observed a correlation between the frequency of the lowest energy CT transition and the energy of the hole in the d_{yz} orbital of the ferric ion in some ligand complexes of metmyglobin and cytochrome c. Unfortunately, because of the limited data set available to them, these workers arrived at an erroneous interpretation of their data. The larger number of examples given in the present work has enabled us to correct their theory.

The near-IR MCD data together with the EPR spectra provide a protocol for the identification of the axial ligands of hemoproteins containing ferric protoporphyrin IX. This method has been used successfully, for example, to follow ligand states of the two hemes in the diheme cytochrome c peroxidase from *Pseudomonas aeruginosa*,[19] to identify the axial ligand changes in the high-pH form of horse heart cytochrome c[20] and in the high-pH form of horseradish peroxidase.[21] The method has also shown that plant cytochrome f has lysine as a second axial ligand,[22] verified that cytochrome b_{558} from *B. subtilis* is coordinated by a pair of histidine ligands,[23] and demonstrated that cytochrome a in bovine cytochrome c oxidase is liganded by two histidine groups.[24] This paper provides a collection of experimental data that should be useful in assisting heme axial ligand diagnosis in proteins.

2. Experimental Section

Electron paramagnetic resonance spectra were recorded with an ER-200D X-band spectrometer (Bruker Spectrospin) interfaced to an ASPECT 2000 computer and fitted with a liquid helium flow cryostat (Oxford Instruments). Magnetic circular dichroism spectra have been measured with a home-built circular dichrograph and a split-coil superconducting solenoid tpye SM-4 (Oxford Instruments) capable of generating a maximum field of 5 T. The sample is held in a boiling liquid helium bath whose temperature can be varied by means of vapor pressure control. The dichrograph has a wavelength range of 0.8–3 μm and a maximum sensitivity of 2×10^{-5} ΔA units. $\Delta A = A_L - A_R$, where A_L and A_R are the absorbances for left and right circularly polarized light, respectively. The instrument is based upon a design originally due to Osborne, Cheng, and Stephens.[25] It consists of a light source and an 0.6-m grating monochromator (Spex Industries) fitted with a grating blazed at 1.6 μm. The white light is chopped at a frequency of 150 Hz. The orders are sorted by filters of red glass, silicon, and germanium. The light emanating from the monochromator is linearly polarized by a calcite Glan prism and passed through a modulator (Hinds International) of calcium fluoride. The modulator produces a beam of left and right circularly polarized light alternating at a frequency of ~50 kHz, which passes through the sample at the center of the solenoid. Calcium fluoride lenses are used to bring the beam to a focus at the sample and to image the monochromator exit slit at the detector. The latter is InSb of large area (10 × 10 mm) cooled to 77 K. The detector has a preamplifier that passes the signal to two lock-in amplifiers tuned to 150 Hz and 50 kHz, respectively. The low-frequency signal is passed to an automatic gain-control circuit, which holds the integrated signal intensity $(A_L + A_R)$ constant at all wavelengths. The high-frequency signal is then proportional to $(A_L - A_R)/(A_L + A_R)$ and gives ΔA directly. The modulator amplitude is varied at intervals throughout the wavelength scan in order to generate circularly polarized radiation at all wavelengths. The instrument is calibrated by two methods. One uses a wave retarder as described,[17] and the other employs a sample of optically active nickel(II) tartrate.[25]

Protein samples have been obtained from a range of sources. Myoglobin was purchased from Sigma, oxidized with $Fe(CN)_6^{3-}$, and purified

(16) Eglinton, D. G.; Johnson, M. K.; Thomson, A. J.; Gooding, P. E.; Greenwood, C. *Biochem. J.* **1980**, *191*, 319–331.
(17) Nafie, L. A.; Keiderling, T. A.; Stephens, P. J. *J. Am. Chem. Soc.* **1976**, *98*, 2715–2723.
(18) Gadsby, P. M. A. Ph.D. Thesis, University of East Anglia, 1984.
(19) Foote, N.; Peterson, J.; Gadsby, P. M. A.; Greenwood, C.; Thomson, A. J. *Biochem. J.* **1985**, *230*, 227–237.
(20) Gadsby, P. M. A.; Peterson, J.; Foote, N.; Greenwood, C.; Thomson, A. J. *Biochem. J.* **1987**, *246*, 43–54.
(21) Foote, N.; Gadsby, P. M. A.; Berry, M. J.; Greenwood, C.; Thomson, A. J. *Biochem. J.* **1987**, *246*, 659–668.
(22) Rigby, S. E. J.; Moore, G. R.; Gray, J. C.; Gadsby, P. M. A.; George, S. J.; Thomson, A. J. *Biochem. J.* **1988**, *256*, 571–577.
(23) Friden, H.; Cheesman, M. R.; Anderson, K. K.; Hederstedt, L.; Thomson, A. J. *Biochim. Biophys. Acta*, submitted for publication.
(24) Eglinton, D. G.; Hill, B. S.; Greenwood, C.; Thomson, A. J. *J. Inorg. Biol.* **1984**, *21*, 1–8.
(25) Osborne, G. A.; Cheng, J. C.; Stephens, P. J. *Rev. Sci. Instrum.* **1973**, *44*, 10–15.

Table I. EPR g Values and Energies of Near-Infrared Charge-Transfer Bands of Low-Spin Ferric Hemoproteins

no.	derivatives	EPR g values[a]			V/λ[b]	Δ/λ[b]	E_{yz}/λ[c]	peak wavelength of near-IR CT band[d] (nm)	E_{CT}/cm^{-1}[d]	$\Delta\epsilon/M^{-1}$ cm^{-1}[e]	ligation of heme[f]
		g_z	g_y	g_x							
					Metmyoglobin						
1	OH^-	2.59	2.17	1.88	3.35	6.88	3.97	1023	9775	102	
2	N_3^-	2.79	2.21	1.72	2.46	4.94	2.88	1290	7752	134	
3	SH^-	2.56	2.24	1.84	3.54	5.09	3.47	1200	8333	94	
4	$SC_3H_7^-$	2.37	2.24	1.93	5.92	5.71	4.86	1035	9662	52	
5	4-methylimidazole, pD 6.6	2.92	2.25	1.54	1.94	3.47	2.08	1506	6646	203	
6	CN^-	3.45	1.89	0.93	0.94	3.36	1.59	1595	6270	594	
7	4-methylimidazole, pD 10.8	2.72	2.25	1.73	2.63	4.29	2.74	1230	8130		
8	imidazole, pD 8.9	2.93	2.22	1.52	1.86	3.53	2.11	1600	6250		
9	imidazole, pD 12.2	2.80	2.25	1.67	2.34	4.04	2.52	1350	7407		imidazolate/His
10	4-nitroimidazole	2.91	2.22	1.52	1.87	3.46	2.09	1475	6780		
11	2-methyl-4-nitroimidazole	2.88	2.27	1.61	2.15	3.72	2.32	1475	6780		
					Leghaemoglobin (soybean)						
12	nicotinate	3.16	2.21	(1.07)[g]	1.26	2.35	1.41	1660	6024	261	
13	OH^-	2.54	2.24	1.84	3.56	4.91	3.42	1060	9434	79	
14	imidazole, pD 6.4	3.03	2.29	1.50	1.87	3.40	2.07	1630	6135	215	
15	imidazole, pD 8.4	2.82	2.29	1.69	2.48	4.05	2.59	1370	7299	205	imidazolate/His
16	1-methylimidazole, pD 8.4	2.98	2.26	1.50	1.86	3.38	2.06	1640	6098	236	
17	*n*-butylamine	3.38	2.05	[1.14][h]	1.17	3.50	1.75	1550	6452	330	
18	phenol	2.65	2.24	1.86	3.68	6.56	4.03	1075	9302	100	
					Leghaemoglobin (Sesbania)						
19	imidazole, pD 7.8	2.89	2.25	1.59	2.07	3.72	2.28	1352	7396	320	imidazolate/His
					Cytochrome *c* (horse heart)						
20	pD 6.6	3.07	2.23	1.26	1.47	2.67	1.63	1750	5714	282	Met/His
21	pD 11.0	3.33	2.05	[1.13][h]	1.17	3.34	1.70	1480	6757	420	Lys/His
22	CN^-	3.47	1.85	(0.73)	0.82	2.86	1.36	1618	6180	645	
23	imidazole	2.96	2.26	1.51	1.88	3.37	2.06	1455	6873	160	
					Cytochrome *c*						
24	tuna	3.11	2.20	1.15	1.33	2.49	1.5	1740	5747	176	Met/His
25	*Candida krusei*	3.18	2.11	1.26	1.35	3.34	1.79	1750	5714	182	Met/His
26	*W. succinogenes*	3.00	2.27	1.43	1.74	3.02	1.88	1508	6631	250	His/His
27	cytochrome c_{551} (*P. aeruginosa*)	3.20	2.06	(1.23)	1.28	3.45	1.79	1800	5555	330	Met/His
28	cytochrome b_{562} (*E. coli*), pD 6.9	3.03	2.18	1.40	1.6	3.33	1.91	1860	5376	176	Met/His
29	cytochrome b_{562} (*E. coli*), pD 10.5	2.79	2.26	1.67	2.37	3.92	2.49	1550	6452	135	Met/His^-
30	heme *a*, bis(imidazole)	2.96	2.29	1.50	1.90	3.18	2.08	1540	6494	310	
31	cytochrome *c* oxidase (cytochrome *a*)	3.03	2.21	1.45	1.70	3.48	2.01	1564	6394	250	His/His
32	cytochrome c_3 (Norway), pD 6.5	3.02	2.25	1.50	1.83	3.56	2.10	1548	6460	234	His/His
33	cytochrome c_3 (*Desulphovibrio vulgaris*), pD 6.5	2.96	2.29	1.59	2.09	3.76	2.3	1502	6658	206	His/His
34	lactoperoxidase–CN	2.96	2.26	1.54	1.94	3.57	2.16	1560	6410	134	CN^-/His

[a] g values ordered as shown. [b] λ is spin–orbit coupling constant of Fe(III). [c] $E_{yz} = \Delta/3 + V/2$; see Figure 1. [d] Peak wavelength of MCD at 4.2K, 5 T; $E_{CT} = 10^7$ (peak wavelength)$^{-1}$. [e] $\Delta\epsilon = \epsilon_L - \epsilon_R$, where ϵ_L and ϵ_R are extinction coefficients for left and right circularly polarized light. $\Delta\epsilon$ value is peak intensity of MCD at 4.2 K and 5 T. [f] Ligation state of heme is indicated in this column in cases where the coordination is not obvious from column 2 of the table. Key: his = histidine; met = methionine; his^- = histidinate. [g] Parentheses indicate g values estimated from relationship $\sum g_i^2 = 16.00$. [h] Brackets indicate that experimental location of g value is uncertain owing to low transition probability or to the possibility of confusion with other signals.

on Sephadex G25. Leghemoglobin *a* (soybean) was a gift from Dr. G. Sievers (Helsinki).

3. Results

The near-IR (MCD) spectra of a wide range of hemoproteins have been recorded both at room temperature and at 4.2 K. In this paper we focus attention upon proteins and model compounds that possess histidine as the proximal, or fifth ligand, and a sixth ligand that can be varied over a wide range of ligand field strengths. The EPR spectrum of every sample has been remeasured at the time of carrying out the MCD experiment. The MCD results reported refer to samples at 4.2 K and in a magnetic field of 5 T. The data are collected in Table I. However, in order to illustrate the forms of the spectra some typical examples are given in Figures 2 and 3. Figure 2 shows the MCD spectra of metmyoglobin complexes with $-SH^-$, $-SR^-$, N_3^-, and CN^-, and of leghemoglobin *a* (soybean) with imidazole and imidazolate. The spectra all have the form of a major peak to longer wavelength that may possess structure and a series of shoulders or partially resolved peaks on the short-wavelength side of the major peak.

In Figure 2 are shown the near-IR MCD spectra of two classes of proteins. Figure 3a shows the spectra of cytochromes coordinated by histidine and methionine. In two cases, horse heart cytochrome *c* and c_{551} from *P. aeruginosa*, the heme group is covalently linked to the polypeptide backbone. In the case of cytochrome b_{562}, *Escherichia coli*, the heme is protoheme IX not covalently linked. The CT band varies in wavelength between 1860 nm, b_{562}, and 1800 nm, c_{551}, and 1750 nm for horse heart *c*. The additional features apparent at ~700 nm correspond to the so-called 695-nm absorption band known to be typical of methionine–histidine coordination. Although these bands are not the subject of this paper, it is interesting to note that the sign of the MCD peaks depends upon the protein.

Figure 3b illustrates the near-IR MCD spectra at 4.2 K and 5 T of three hemoproteins with bis(histidine) coordination, namely, cytochrome c_3 at 1548 nm, cytochrome *c* (*Wolinella succinogenes*) at 1508 nm, and cytochrome *b* associated with formate dehydrogenase (*P. aeruginosa*). The preparation of the cytochrome *b* contains a minor impurity of a methionine–histidine coordinated heme, visible at ~1850 nm. The near-IR MCD of model bis(imidazole)-coordinated ferric octaethylporphyrin have been reported,[26] showing wavelengths of the main peak in the range 1540–1610 nm.

(26) Gadsby, P. M. A.; Thomson, A. J. *FEBS Lett.* **1986**, *197*, 253–257.

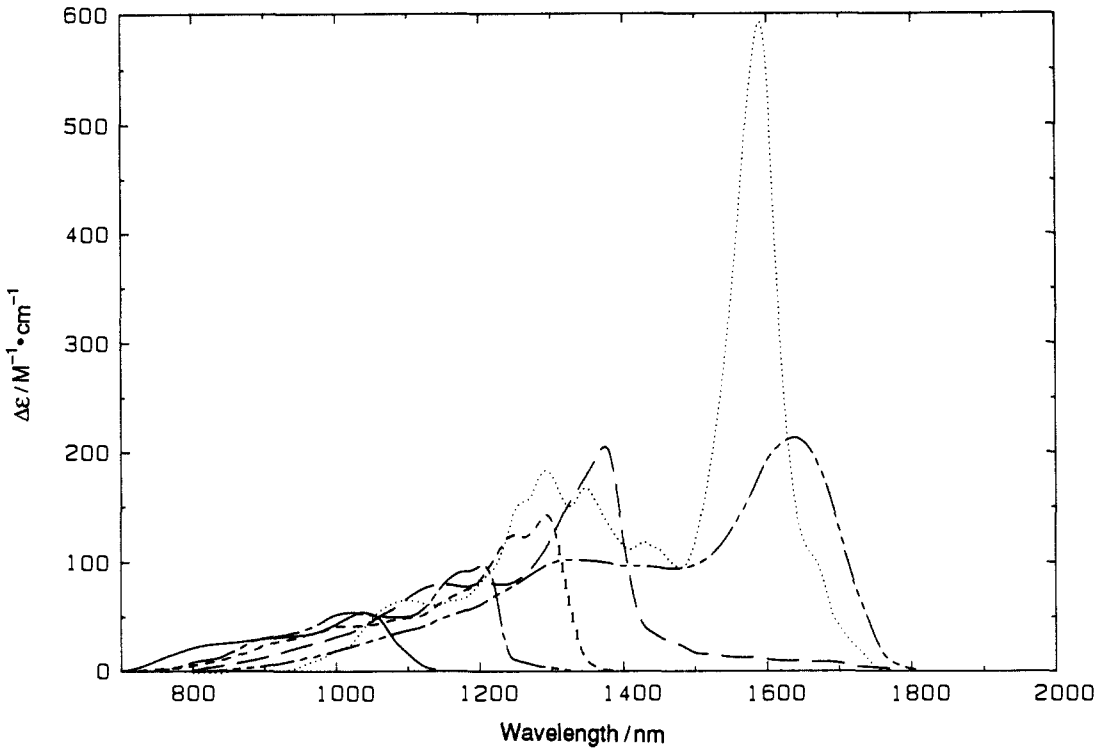

Figure 2. Near-infrared MCD spectra of ferric heme adducts of metmyoglobin and metleghemoglobin (soybean). Spectra recorded at 4.2 K and 5 T. Key: (—) metMb–SC_3H_7 (**4**), (—·—) metMb–SH (**3**), (---) metMb–N_3 (**2**), (– – –) Lb–imidazolate (**15**), (···) metMb–CN (**6**), and (–··–) Lb–imidazole (**14**). Numbers in parentheses refer to Table I. The conditions for each protein are given in the original references.

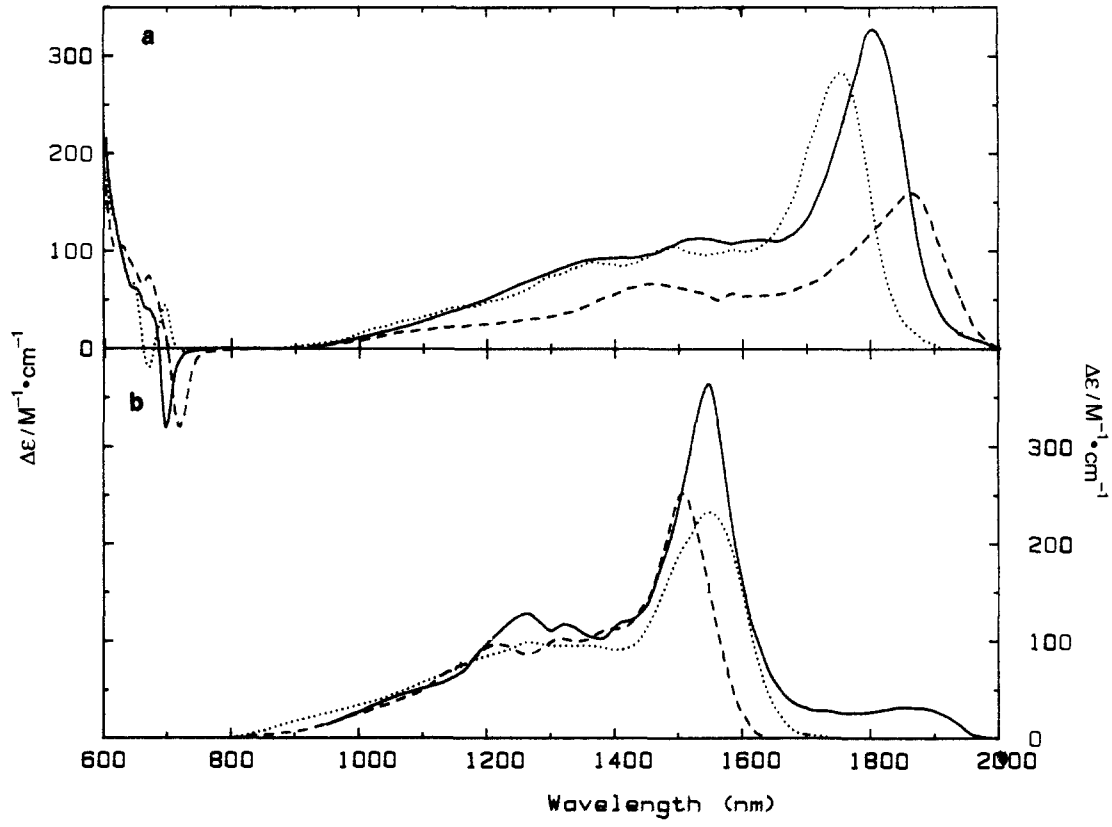

Figure 3. Near-infrared MCD spectra of oxidized cytochromes recorded at 4.2 K and 5 T. (a) Methionine–histidine ligation: (···) horse heart cytochrome *c* (**20**), (—) cytochrome c_{551} (*P. aeruginosa*, **27**), (---) cytochrome b_{562} (*E. coli*, **28**). (b) Histidine-histidine ligation: (···) cytochrome c_3 (Norway, **32**), (—) cytochrome b_1 from formate dehydrogenase (*P. aeruginosa*),[44] (---) cytochrome *c* (*W. succinogenes*).[26] The numbers in parentheses refer to the list in Table I.

The complete collection of data is given in Table I. The EPR *g* values quoted are used to calculate, by means of Taylor's formula,[3] the axial (Δ) and rhombic (V) distortion parameters. Note that a right-handed Cartesian coordinate system with origin at Fe(III) has been assumed. The axis system is taken to be fixed and is allowed to become "improper" according to the definition of Taylor.[3] Hence, V/Δ ratios of greater than 2/3 may be found. The peak wavelength of the near-infrared charge-transfer band

is also expressed in nanometers and as E_{CT} in reciprocal centimeters. The intensity of the major peaks in the MCD spectrum, $\Delta\epsilon$, at 4.2 K and 5-T field is also quoted. The data gathered in Table I are restricted to those ferric hemoproteins for which all three rhombic components of the **g** tensor are detectable. Hence, the crystal field parameters V and Δ are unambiguously determined in units of λ.

The data in Table I show that the energy of the near-IR CT band varies from 5370 to 10000 cm^{-1} as the second axial ligand of the heme is varied from methionine to a hydroxyl or phenolate group. This wide variation in energy provides a useful spectroscopic ruler of the axial ligation state of the heme groups and enables any ligation changes to be followed with ease.

A further striking feature of the spectra is the wide variation in intensity at 4.2 K and 5 T of the MCD bands. For example, $\Delta\epsilon$ varies from 550 M^{-1} cm^{-1} for metMb–CN to 52 M^{-1} cm^{-1} for metMb–SC_3H_7. It has been shown elsewhere[45] that there is a correlation between $\Delta\epsilon$ and V, the rhombic distortion parameter, determined from the EPR g values, and that a simple model of the CT intensity provides an explanation of this empirical correlation.

In the next section we explore the relationships between the variation of the energy of the near-IR CT band, E_{CT}, and the energy of the hole in the t_{2g} orbital, as determined by EPR spectroscopy.

4. Energy of Hole and Charge-Transfer Transitions

The one-electron orbital energies of the porphyrin ring and ferric ion are shown in Figure 1. The highest filled porphyrin orbitals are of symmetries a_{1u} and a_{2u}, and the lowest empty orbitals have the symmetry e_g, classified under tetragonal (D_{4h}) symmetry. The ferric ion d orbitals are split in energy by the field of the four in-plane pyrrole nitrogen atoms of the porphyrin ring and by the basal and apical axial ligands. If all six ligands were equivalent, a splitting of the d orbitals into two subsets, labeled e_g and t_{2g} under the point group O_h, would result. However, in a lower symmetry field the d shell is further split so that the orbital degeneracy of the t_{2g} subshell is completely lost. The five d electrons of the low-spin ferric ion occupy the three lowest energy levels, leaving a hole in the d_{yz} orbital.

The charge-transfer transitions observed in the near-IR are from the highest filled porphyrin π orbitals, a_{1u} and a_{2u}, to the hole in the t_{2g} subshell of the ferric d orbitals. Hence, the energy of the transition, E_{CT}, is dependent on the energy of the positive hole on the ferric ion relative to that of the highest filled porphyrin radicals.

The EPR signals arise from the odd electron in the t_{2g} orbital. The anisotropy of the **g** tensor is due to the combined effect of axial and rhombic low-symmetry crystal fields and spin–orbit coupling that mixes the three d orbitals of the t_{2g} subshell. In this work we follow the analysis of Taylor.[3] Knowledge of the three g values enables the two energy parameters Δ and V in units of the spin–orbit coupling constant (λ) to be determined. These parameters describe the axial and rhombic splittings of the one-electron orbitals as shown in Figure 1. Table I lists the parameters for all the hemoproteins studied here. The energy E_{yz} of the d_{yz} hole relative to the center of gravity of the t_{2g} subset of orbitals is given by $(2\Delta + 3V)/\lambda$. This quantity is given in the table.

The energy level diagram (Figure 1) shows that a correlation will exist between the energy of the near-IR CT band, E_{CT}, and the energy of the hole in the t_{2g} subset for a given series of ligands provided that a number of factors remain approximately constant throughout the series.

Eaton and Schejter[13] first tried to demonstrate such a correlation by making the assumption that the energy of the d_{xy} orbital relative to that of the filled porphyrin orbitals, $a_{1u}(\pi)$ and $a_{2u}(\pi)$, stayed constant. The energy of the CT band was expressed in terms of one-electron orbital energies as

$$E_{CT} = C_{JK} + E(d_{xy}) - E(a_{1u}) + \lambda(\Delta + V/2)/\lambda$$

where C_{JK} contains the Coulomb and exchange terms. A linear relationship between E_{CT} and $(\Delta + V/2)/\lambda$ is predicted with a slope equal to the spin–orbit coupling constant λ.

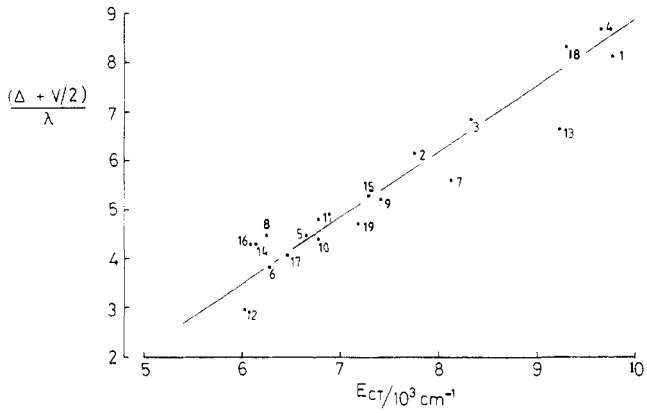

Figure 4. Plot of $(\Delta + V/2)/\lambda$, the energy separation between the d_{yz} and d_{xy} orbitals, versus E_{CT}, the energy of the near-infrared charge-transfer band. The numbered points refer to Table I. The solid line represents a least-squares fit, with a correlation coefficient of 0.91, to the equation $E_{CT} = 3423 + 741(\Delta + V/2)/\lambda$. This demonstrates the correlation first proposed by Schejter and Eaton.[13]

A plot of the data for derivatives **1–9** listed in table I is given in Figure 4. A linear least-squares fit to these points gives the equation

$$E_{CT} = 3423 + 741(\Delta + V/2)/\lambda$$

The correlation coefficient is 0.91. The slope obtained is 741 ± 58 cm^{-1}. This is large by a factor of 2 for the spin–orbit coupling constant of ferric ion, which has a value of 460 cm^{-1} in the free ion. This shows that the energy of the charge-transfer band shifts more rapidly than does the separation between the d_{xy} and $d_{xz,yz}$ orbitals.

This conclusion is contrary to that arrived at by Eaton and Schejter.[13] The data examined by these authors consisted of only eight points, which agree with the data in Table I except for one point, that for cytochrome c in 1 N NaOD. The EPR of the product was not measured by Schejter and Eaton. Instead, assignment to the hydroxide form of cytochrome c was assumed, and g values of 2.56, 2.18, and 1.85 were taken from ref 2. However, this assignment is uncertain, given the number of low-spin species that are present in cytochrome c at high pH.[20] This data point is at the extreme of the plot and has a large effect on the slope. If this point is discarded, Eaton and Schejter's plot gives a slope of 800 cm^{-1}, close to that determined here. Therefore, it appears that the assignment of this species is in error, which in turn leads to an incorrect estimate of the slope and, hence, to an erroneous conclusion.

These results show that although E_{CT} is correlated with the overall energy separation of d_{xy} and d_{yz}, the d_{xy} orbital energy does not remain unchanged as heme axial ligands are altered. We examine a second hypothesis, namely that the energy of the baricenter of the t_{2g} orbitals remains constant relative to that of the filled porphyrin orbitals. We plot E_{yz}, the energy of hole relative to the center of gravity of the t_{2g} subset, against E_{CT} (Figure 5). The plot shows a clear correlation between these two parameters. Nineteen of the derivatives (points **1–19**) consist of complexes of metmyoglobin and Lba, the sixth ligand being a range of exogenous ligands. A linear least-squares fit to these points gives the equation

$$E_{CT} = 3973 + 1322E_{yz}/\lambda$$

The correlation coefficient is 0.89, and the slope is 1322 ± 114 cm^{-1}.

Also included in Figure 5 are points for proteins with different heme rings. **20–26** are derivatives of cytochrome c in which the heme is covalently bound to the protein. The parameters from cytochrome b_{562} (*E. coli*) and cytochrome c_3 (*D. vulgaris*, and Norway strain) are also included. All these points lie at the lower end of the plot. A least-square fit of **1–34** changes the equation only slightly to

$$E_{CT} = 3742 + 1369E_{yz}/\lambda$$

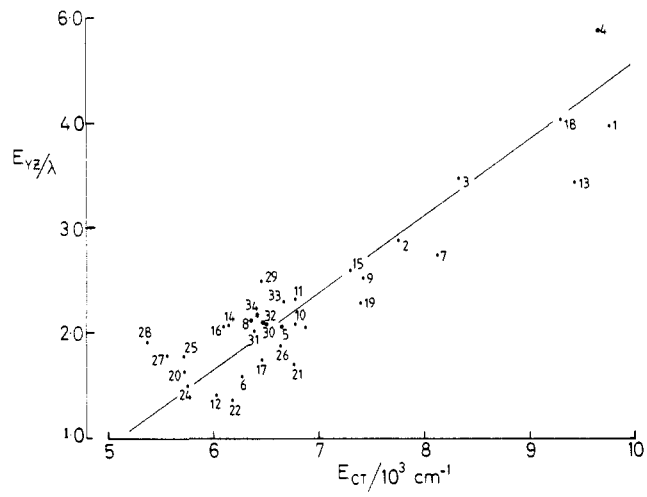

Figure 5. Plot of the energy, E_{yz}, of the d_{yz} hole relative to the baricenter of the d-orbital t_{2g} subshell versus E_{CT}, the energy of the near-infrared CT band. The numbered points refer to Table I. The solid line represents a least-squares fit with a correlation coefficient of 0.85 to the equation $E_{CT} = 3742 + 1369E_{yz}/\lambda$.

The correlation coefficient is 0.85, and the slope is 1369 ± 102 cm^{-1}. Taking a value of 400 cm^{-1} for the spin–orbit coupling constant yields a slope of ~3.3. Therefore, the energy shift of the charge-transfer band is over 3 times greater than the change in the energy of the hole relative to the baricenter of the t_{2g} orbitals. Assuming that the energies of the porphyrin orbitals, $a_{1u}(\pi)$ and $a_{2u}(\pi)$, are independent of the heme axial ligands, the above relationships imply that the energy of the t_{2g} baricenter is changing as the axial ligands are varied. This is not surprising since the sixth axial ligand contributes to the overall crystal field experienced by the Fe(III) ion.

This assumption is valid to a good approximation for protoheme IX, whether covalently or noncovalently bound to a polypeptide chain. The α band, corresponding to a mixture of the one-electron transitions $a_{1u}(\pi)$ and $a_{2u}(\pi)$ to $e_g(\pi^*)$, is little changed in energy by variation in axial ligation provided that the heme remains low spin. However, partially reduced porphyrin rings such as heme d_1, dioxoisobacteriochlorin, have α bands shifted away from the region 550–570 nm to above 600 nm. No CT bands have been detected in the near-IR MCD spectroscopy between 800 and 2000 nm. (Peterson, J.; Thomson, A. J.; Sutherland, J.; Greenwood, C. Unpublished work.) Hence, it appears that large shifts in the energy of the a_{1u} and a_{2u} orbitals by changes in peripheral porphyrin ring substitution can shift the CT bands significantly. The treatment proposed in this paper applies to porphyrin ring systems in which the optical properties approximate to a 4-fold axis along the heme normal. Rings with large distortions from the equivalence of x and y are excluded. Much more MCD work locating the energies of the CT states of reduced porphyrin ring systems, including siroheme and chlorins, needs to be undertaken.

Figures 4 and 5 show that the second axial ligands can be arranged in an empirical order of increasing E_{CT}, E_{yz}, and Δ thus: thioether < CN^- ~imidazole ~RNH_2 < imidazolate < N_3^- < SH^- < phenolate ~OH^- ~RS^-.

This does not correspond closely to the order of these ligands in the spectrochemical series. For example, CN^- and thioether are adjacent in the order, whereas they are at opposite ends of the spectrochemical series. Since E_{CT} is empirically correlated with the splitting of the t_{2g} subshell, it is the ability of the axial ligand to bring about an axial distortion that is likely to be of importance.

The crystal field strength at the iron is provided by the four in-plane nitrogen atoms of the porphyrin ring, the fifth nitrogen ligand of the histidine axial ligand, and the sixth ligand, which is varied throughout the series. Thus, the average crystal field depends upon the sixth ligand. The axial distortion, however, depends upon the difference between the crystal field strengths of the basal and the apical ligands. In the following paragraphs the relationship between the axial field and the average octahedral crystal field is examined.

The d-orbital energies relative to the baricenter of the 3d shell are given by

$$E_{xz,yz} = 4Dq - Ds - 4Dt$$
$$E_{xy} = 4Dq - 2Ds - Dt$$
$$E_{z^2} = 6Dq - 2Ds - 6Dt$$
$$E_{x^2-y^2} = 6Dq - 2Ds - Dt \quad (1)$$

Ds and Dt are second- and fourth-order radial integrals of the 3d shell.[27] Changes in Ds are centered about the t_{2g} and e_g subshells, whereas changes in Dt occur around the total d-orbital configuration. The parameters Dq, Ds, and Dt can be expressed as sums of (or differences between) the contribution from the equatorial and axial ligands,[28] thus

$$Dq = \tfrac{2}{3}Dq^e + \tfrac{1}{3}Dq^a$$
$$Ds = Ds^e - Ds^a$$
$$Dt = \tfrac{4}{7}(Dq^e - Dq^a) \quad (2)$$

where the superscripts e and a refer to the contributions to the radial integrals from the equatorial and axial ligands. From eq 1 and 2 it is possible to express the tetragonal distortion of the t_{2g} subshell in terms of the difference between the radial parameters of the in- and out-of-plane ligands since the equatorial parameters Ds^e and Dq^e are invariant throughout the series

$$E_{yz} = \frac{\Delta}{3} = \text{constant} - Ds^a + {}^{20}\!/_{21}Dq^a \quad (3)$$

where the constant contains the equatorial crystal field parameters.

The energy of the charge-transfer transition can be written as

$$E_{CT} = K - 4Dq + \frac{\Delta}{3} \quad (4)$$

where K contains the energy gap between the $a_{1u}(\pi)$ orbital of the porphyrin ring and the baricenter of the d orbitals, plus interelectron repulsion parameters. These two terms are taken to remain constant for all the heme derivatives studied here. This is cearly not rigorously true. However, the changes involve only one of six ligands of the ferric ion.

On this assumption, E_{CT} can be expressed in terms of the axial radial parameters with eq 2–4 giving the result

$$E_{CT} = K' - Ds^a - {}^{8}\!/_{21}Dq^a \quad (5)$$

K' contains both K and Ds^e and Dq^e, all constant. Equation 5 shows that E_{CT} *increases* as the crystal field parameters of the axial ligand *decreases*, provided that the second two terms on the RHS of eq 5 are smaller than K'. A *linear* relationship between E_{yz} and E_{CT} can be obtained only if the parameters Ds^a and Dq^a have a fixed ratio independent of the axial ligand. Writing $\tau = Dq^a/Ds^a$, an expression relating E_{CT} and E_{yz} can be written

$$E_{CT} = K' + E_{yz}\frac{29}{\tau} \quad (6)$$

The experimentally observed plot of E_{CT} versus E_{yz} (Figure 5) suggests that τ does remain approximately constant across the series of complexes studied in this work.

Much consideration has in the past been given to the evaluation of the radial integrals Ds and Dq.[28] Ballhausen and Ancmon[29] have shown that the ratio of the two is a relatively slowly varying function of parameters such as metal–ligand bond lengths and

(27) Ballhausen, C. J. *Introduction to Ligand Field Theory*; McGraw-Hill Book Co.: New York, 1962; p 101.
(28) Gerloch, M.; Slade, R. C. *Ligand Field Parameters*; Cambridge University Press: New York, 1973.
(29) Ballhausen, C. J.; Ancmon, E. M. *Mat-Fys. Medd.-K. Dan. Vidensk. Selsk* **1958**, *31*, 2.

effective nuclear charges. Hence, we conclude that the empirical correlation of Figure 5 is reasonably well accounted for by eq 6.

5. Discussion

Near-infrared MCD spectroscopy provides a reliable method of locating the long-wavelength porphyrin to ferric CT transitions of low-spin ferric hemoproteins. When the sample is held at liquid helium temperatures, a considerable gain in sensitivity is achieved because the MCD intensity is inversely proportional to the absolute temperature, in the linear field regime. This is important in some cases since the absorption intensities of these transitions are relatively weak with ϵ values of the order of 200 M^{-1} cm^{-1} at room temperature. The MCD spectra have been measured at low temperatures in order to ensure that the sample conditions are the same as those used for the measurement of the EPR spectra. The EPR signals of the low-spin ferric hemes can be detected only at low temperatures. The measurement of MCD spectra at liquid helium temperatures requires the addition of a cryoprotectant to generate optical glasses of satisfactory optical quality. Our work invariably uses ethanediol or glycerol. The EPR spectra have been recorded in all the cases given in Table I from the same solutions as those used for the measurement of MCD spectra, that is, in the presence of a glassing agent. In all cases only a single low-spin ferri heme species has been detected by EPR spectroscopy. Near-IR MCD spectroscopy has the advantage over EPR spectroscopy in that the spectra can also be readily measured at room temperature. Therefore, measurement of the near-IR MCD spectrum at room and low temperature enables species detected by low-temperature EPR spectra to be identified. Changes in axial ligation on freezing of samples are not uncommon in proteins. These processes are most readily correlated with axial ligation changes with near-IR MCD spectroscopy at several different temperatures. In this paper we seek to show the relationship between the "truth" table method of axial ligand assignment with EPR g values and the use of near-IR MCD spectroscopy.

By collecting the data on 34 different examples, we have investigated the utility of using the wavelength of this transition as an aid to the diagnosis of axial ligand type. It is clear that there is a correlation between the energy of the charge-transfer transition, E_{CT}, and the energy of the hole on the ferric ion, E_{yz}, as determined from EPR spectroscopy. The crucial question to consider is how unambiguously can the nearIR MCD spectrum of a low-spin ferric hemoprotein diagnose axial ligand coordination? The truth table devised by Blumberg and Peisach[1] was the first method to use spectroscopic parameters to suggest assignments of the axial ligand pairs of low-spin ferric hemoproteins. The method relied upon the calculation of V and Δ from the **g** tensor and the observation that Δ particularly varies between axial ligand pairs. Variations in V, the rhombic parameter, occur for a given axial ligand set. It is now becoming clear in some cases that this can be brought about by the protein inducing twist in the relative orientation of the axial ligands. The present work has shown that E_{CT} and the EPR parameters V and Δ are closely correlated, via the energy of the hole $E_{yz} = (\Delta/3 + V/2)/\lambda$ (Figure 5). Hence, the two methods of ligand assignment, namely the truth table and the energy of the near-IR CT band, are not independent of one another.

A diagrammatic representation of the power of the two methods to discriminate between ligand types is shown in Figure 6. This summarizes selected data from Table I. We consider five different axial ligation states that have been studied here. They are methionine–histidine, histidine–histidine (or histidine–imidazole, which is taken to the equivalent), histidine–histidinate (or imidazolate), methionine–histidinate, and thiolate–histidine. The separation between the points for groups of proteins of the same ligation state is greater for E_{CT} than for E_{yz} because the energy spread is larger in the former. The response of E_{CT} to changes in E_{yz} is greater by a factor of about 3.3.

Methionine–histidine coordination generates a CT band in the range 1740 nm (tuna cytochrome *c*) to 1950 nm (*A. vinelandii* cytochrome c_4). This ligation state is the most clear to diagnose by MCD spectroscopy. Not only are the near-IR CT bands well

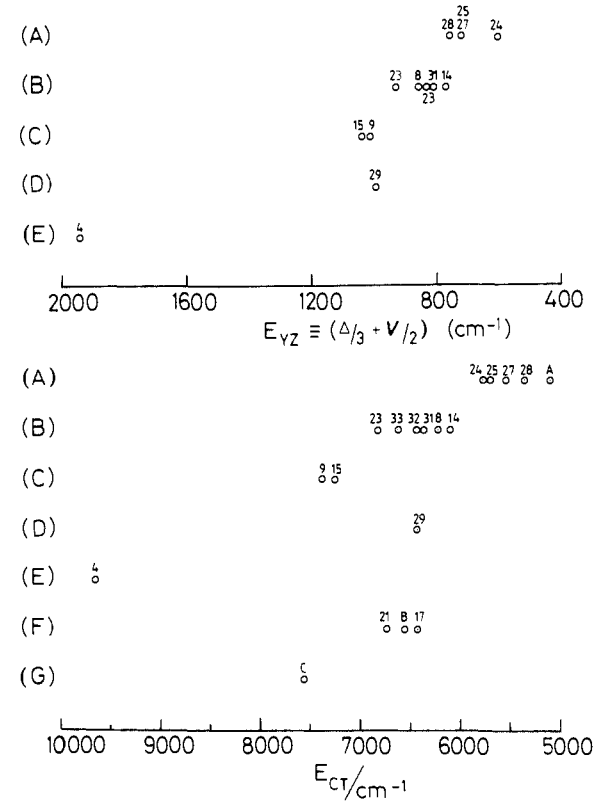

Figure 6. Comparison of the energy of the hole, E_{yz}, in low-spin ferric ion hemes relative to the energy of the near-infrared CT band, E_{CT}, for various axial ligation states of low-spin ferric hemes. E_{yz} is determined from the EPR g values and E_{CT} from the near-IR MCD spectra. Key: (A) methionine–histidine, (B) histidine–histidine, (C) histidine–histidinate, (D) methionine–histidinate, (E) thiol–histidine, (F) lysine (or amine)–histidine, and (G) amine–amine. The points numbered refer to Table I. Point A is cytochrome c_4 (*A. vinelandii*), point B is cytochrome *f* (woad, charlock, rape), and point C is bis(*n*-butylamine) (octaethylporphyrin)iron.

separated from that of other known ligation states but also confirmatory evidence is provided by observation of a distinctive band at about 695 nm. This band also varies in wavelength depending upon the nature of the protein. The MCD spectrum locates it readily at low temperatures when the band is a rather well-resolved negative or positive band. This transition has been assigned as a methionine–sulfur to ferric(III) CT band.[30] Single-crystal spectra have shown it to be polarized predominantly perpendicular to the heme plane. However, to appear in the MCD spectrum, the band must contain some intensity component perpendicular to this.

Bis(histidine) coordination leads to a near-IR CT band at 1502 nm in cytochrome c_3 (*Desulphovibrio vulgaris*) and 1558 nm in c_3 (*Desulphovibrio*, Norway). Imidazole–histidine and bis(imidazole) coordination gives rise to bands at similar wavelengths as the imidazole derivatives of Mb and leghemoglobin (Lb) show. The wavelength range is slightly larger, being 1630 nm for imidazole–Lb and 1600 nm for imidazole–metMb. Heme *a* bis(imidazole) gives a band at 1540 nm, and cytochrome *a* in bovine cytochrome *c* oxidase shows a peak at 1564 nm. The latter result was the clearest evidence that the low-spin cytochrome *a* is bis(histidine) ligated.[24,31] This shows that the heme *a* ring system gives near-IR CT bands at energies similar to those of protoheme IX derivatives. Thus, although the 8-formyl group of the heme *a* ring affects the visible region spectrum of the heme to a marked extent, it does not affect the Fe(III) d-orbital energies or the highest filled porphyrin π orbitals.

(30) Eaton, W. A.; Hochstrasser, R. M. *J. Chem. Phys.* **1967**, *44*, 2533–2539.
(31) Thomson, A. J.; Eglinton, D. G.; Hill, B. C.; Greenwood, C. *Biochem. J.* *207*, 167–170.

Ligation by the histidinate group, or imidazolate, in which the N-1 proton of the histidine (or imidazole) ring is lost can be readily diagnosed via the near-IR CT bands. Indeed, such experiments led to the unambiguous diagnosis of N-1 proton loss in imidazole complex of Lb[32] and in cytochrome b_{562} (*E. coli*).[33] The N-1 deprotonated form of coordinated imidazole in metMb above pD 12.2, in Lb*a* (soybean) above pD 8.4 and in Lb (sesbania)[34] at pD 7.8, have near-IR CT bands at 1350, 1370, and 1358 nm, respectively, whereas the protonated forms yield peaks at 1600 and 1630 nm in the first two cases. The protonated state of the sesbania Lb–imidazole complex has not been observed. The shifts on deprotonation are 1050 cm^{-1} for metMb–imidazole and 1164 cm^{-1} for Lb–imidazole; see Figure 6. The deprotonation of proximal histidine ligand has been established in cytochrome b_{562} (*E. coli*).[33] This cytochrome possesses methionine–histidine coordination as established by X-ray crystallography. The near-IR CT band moves from 1860 and 1550 nm on deprotonation, an energy shift of 1076 cm^{-1}; see Figure 6. Hence, the shift is approximately constant, in energy terms, on loss of a proton from the N-1 of imidazole or histidine, being a blue shift of the CT band between ~1080 cm 1170 cm^{-1}. This is consistent with the higher crystal field strength of the deprotonated state compared with the protonated form.

The near-IR CT band of the high-pH form, histidine-deprotonated state, of cytochrome b_{562} (*E. coli*) lies at 1550 nm in the middle of the region of the bis(histidine) bands (Figure 6). There is, however, no ambiguity in ligand assignment. Coordination by methionine–histidine gives rise to a methionine–Fe(III) CT band, the counterpart of the 695-nm band. This band is also blue shifted on deprotonation of the histidine ligand and is very clear in the low-temperature MCD spectrum as a negative trough at 720 and 680 nm.[33] This band is not so evident in the absorption spectrum since on deprotonation the blue shift takes the band under the tail of the more intense α band. Indeed, this band was overlooked in the early study of cytochrome b_{562}, and this led to a misassignment of axial ligation in this, the high-pH form of the protein.[35] The blue shift of this band is 800 cm^{-1}. A simple one-electron model predicts that the two CT bands, at 1860 and 720 nm, should move by about the same energy since in both cases the acceptor orbital is the hole on the Fe(III) ion.

It is important to exphasize that our protocol for axial ligand assignment of heme requires measurement of *both* EPR and near-IR MCD spectra. Although the two techniques are linked as Figure 6 demonstrates, they do provide vital complementary information. For example, the loss of proton from the N-1 position of coordinated histidine or imidazole is a case in point. The change from the protonated to the deprotonated state leads to changes in the **g** tensor as follows. In the case of imidazole–metMb, the *g* values shift from 2.94, 2.22, and 1.52 to 2.80, 2.75, and 1.67 on proton loss; for imidazole–Lb*a* (soybean) the corresponding changes are 3.03, 2.29, and 1.59 to 2.82, 2.29, and 1.69. The data for cytochrome b_{562} illustrate the same shifts from the low-pH form 3.03, 2.12, and 1.40 to 2.79, 2.26, and 1.67. Hence, these changes, together with observation of a blue shift of the near-IR CT band of ~1100 cm^{-1}, are good evidence for deprotonation of the coordinated histidine group.

The ability to be able to follow such deprotonation processes, in bis(histidine)-coordinated hemes at room temperature, promises to be valuable in deciding between models of redox-linked proton release and uptake processes, especially in membranous proteins such as cytrochrome *c* oxidase and the *b*-type cytochromes.

Thiolate–histidine coordination has been modeled in this work with SH^- and $C_3H_7S^-$ derivatives of metMb, which give near-IR CT bands at 1200 and 1035 nm, respectively. The *g* values of 2.56, 2.24, and 1.84 and 2.37, 2.24, and 1.93 are characteristic also. Both techniques discriminate well between this coordination state and others (Figure 6). It will be of interest to see how these wavelengths relate to those found in derivatives of cytochrome P-450 and chloroperoxidase, two naturally occurring proteins known to contain thiolate as axial ligands.[36]

Hence, discrimination between methionine–histidine, bis(histidine), and thiol–histidine is unambiguous with near-IR MCD. Deprotonation of a histidine group is also clearly observed by near-IR MCD and EPR spectra when the change in the protonation state can be observed. The diagnosis of amine–histidine coordination is less clear-cut and can be confused with bis(histidine) coordination. The examples available are the butylamine adduct of Lb*a* (soybean), the high-pH form of horse heart cytochrome *c*, and cytochrome *f* (from woad and charlock). The wavelengths are 1550, 1480, and 1520 nm, respectively (Figure 6). These wavelengths fail to discriminate sharply between the bis(histidine) coordination and amine–histidine. However, in combination with EPR spectroscopy the assignment becomes less ambiguous. The *g* values for the three examples quoted are 3.38 and 2.05 (1.14), 3.33 and 2.05, (1.13), and 3.55 and 1.7 (?). The g_z value is greater than that observed for bis(histidine) coordination in most cases. There are examples of bis(histidine) coordination in which g_z values rise above 3.5, but in this case the line shape becomes non-Gaussian, with a sharp cut off on the low-field edge giving a ramp-shaped appearance to the line shape. In the case of aminohistidine coordination, such as cytochrome *f*, the g_z value at 3.55 has a perfectly Gaussian shape.[22] Hence, differentiation between amine–histidine and histidine–histidine coordination is not unambiguous with near-IR MCD spectroscopy alone. When taken together with the evidence of EPR *g* factors and especially the line shapes of the g_z value, a conclusion can be drawn. However, this is the ligand pair least certain of assignment by this method, and due caution is needed in arriving at a conclusion. Additional evidence, from sequence data for example, should be used wherever possible.

The data gathered together here refer almost exclusively to protoheme IX coordinated by a proximal histidine ligand. Other proximal ligand states now known by X-ray crystallography are cysteinethiol, in cytochrome P-450-CAM,[37] and phenolate of tyrosine in catalase.[38] No examples are yet known of coordination by the amine of lysine in the proximal position. Consideration must be given to the possibility of proteins being discovered with bis(thiol), bis(phenolate), bis(amine), or bis(thioether) coordination of the heme group. Bis(phenolate) is unlikely to lead to the low-spin state of ferric heme. Neither bis(cysteinate) nor bis(methionine) coordination of a heme group has been reported in a protein. However, model bis(thiolate) complexes of ferric porphyrin have been studied by EPR spectroscopy, although not by near-IR MCD. The *g* values for Fe^{III}TPP–bis(isoarylthiolate) complex are 2.273, 2.191, and 1.989,[39] with other thiolate complexes having similar values. Therefore, this coordination should be recognizable from an EPR spectrum alone. Somewhat surprisingly, bis(thioether) coordination of Fe^{III}TP leads to formation of a low-spin complex, at least at 10 K. The *g* values reported are 2.91 and 2.37. Since these overlap the range of values obtainable from methionine–histidine and histidine–histidine coordination, further experimental criteria are needed. No optical or MCD data have been reported for bis(thioether) coordination.[46] A model for bis(amine) coordination has been reported, namely, the complex of bis(*n*-butylamine)ferric octaethylporphyrin.[26] This gives a near-IR CT band at 1320 nm and *g* values of 3.69 and 1.69. The spectra are quite distinct among those given in Table I; see Figure 6. The wavelength of the near-IR CT band does not distinguish the species from, for example, histidine–histidinate

(32) Sievers, G.; Gadsby, P. M. A.; Peterson, J.; Thomson, A. J. *Biochim. Biophys. Acta* **1983**, *742*, 637–647.
(33) Moore, G. R.; Williams, R. J. P.; Peterson, J.; Thomson, A. J.; Mathews, F. S. *Biochim. Biophys. Acta* **1985**, *829*, 83–96.
(34) Gadsby, P. M. A.; Thomson, A. J.; Appleby, C. A. Unpublished data.
(35) Myer, Y. P.; Bullock, P. A. *Biochemistry* **1978**, *17*, 3723–3729.
(36) Dawson, J. H. *Science* **1988**, *240*, 533–439.
(37) Poulos, T. L.; Finzel, B. C.; Gunsalus, I. C.; Wagner, G. C.; Kraut, J. *J. Biol. Chem.* **1985**, *260*, 16122–16130.
(38) Fita, I.; Rossmann, M. G. *J. Mol. Biol.* **1985**, *185*, 21–37.
(39) Byrn, M. P.; Katz, B. A.; Keder, N. L.; Levan, K. R.; Maguramy, C. J.; Melks, K. M.; Pritt, J. W.; Strouse, C. E. *J. Am. Chem. Soc.* **1983**, *105*, 4916–4922.
(40) Mashiko, T.; Reed, C. A.; Haller, K. J.; Kastner, M. E.; Scheidt, W. R. *J. Am. Chem. Soc.* **1981**, *103*, 5758–5767.

coordination, although the g value does. The g_z value at 3.69 is Gaussian in shape in spite of its close approach to the cut-off value of $g_z = 4.0$ for low-spin ferric heme.

Clearly a wider range of examples of ligation states involving thiols, thioethers, and amines particularly are required in order to give the method wider scope. Model complexes usually provide the most direct way to gather more points for the correlation. The recent suggestion that the guanidinum side chain of arginine can become a ligand in place of the proximal histidine residue of cytochrome *c* is quite unexpected[41] and remains to be confirmed by spectroscopy.

Throughout, we have stressed the importance of having both the EPR and the near-IR CT band data for low-spin ferric hemes for more secure axial ligand assignment. This is especially so when the heme complex experiences a crystal field of low rhombicity and high axiality. In this case, much discussed recently,[7] the g_z value moves around $g \sim 3.5$, and the other two components of the **g** tensor are invariably undetectable because they are so broad. In this case the MCD method can be invaluable. We quote some illustrative examples here. Cytochrome c_4 (*A. vinelandii*) contains two covalently bound hemes with reduction potentials of 263 and 317 mV. The two hemes are distinguished in the low-temperature EPR spectra by two sets of low-spin **g** tensors at 3.22, 2.14 (1.17) and at 3.64.[42] The latter signal has a folded line shape, and the other two **g** tensor components could not be detected. The near-IR MCD spectrum shows a CT band at 1940 nm for both hemes, enabling the assignment of methionine–histidine coordination to both hemes. This result is quite consistent with the sequence data. The EPR spectrum is unusual. The observation of a methionine–histidine-coordinated heme with $g_z = 3.64$ and a folded line shape is unexpected and reopens the question of the axial ligand assignment of cytochromes such as b_{568} (yeast) ($g = 3.76$) and b_{562} (yeast) ($g = 3.60$).

This paper has been concerned with spectroscopic methods of axial ligand assignment in the case of low-spin ferric hemes with ligands that are provided by the protein as amino acid side chains. However, in the case of high-spin ferric heme the method can also be used in the following way. Addition of cyanide ion invariably will bind to the sixth coordination site, causing the heme to switch to low spin. A set of data on cyanide-bound hemes then provides a method of diagnosing the proximal axial ligand. Table I shows that a CN^-–histidine-coordinated heme has a near-IR CT band at 1595 nm (CN–metMb), 1618 nm (CN–cytochrome *c*), and 1560 nm (CN–lactoperoxidase), whereas the g_z values vary from 3.45, 3.47 to 2.96, respectively. In partially reduced cyanide adduct of bovine cytochrome *c* oxidase, the near-IR MCD CT band lies at 1545 nm and a g_z value of 3.40 is observed. This showed that cytochrome a_3, the binding site for CN^-, has histidine as its proximal ligand.[43] However, in the fully oxidized form of the cyanide adduct of the enzyme, the near-IR CT band is detected at 1946 nm.[31] The shift in CT band is due to ligation of the nitrogen end of CN^- by copper(II), so-called $copper_B$, so that a bridge between the heme of cytochrome a_3 and $copper_B$ takes place, thus $Fe(III)–C{\equiv}N–Cu_B(II)$. The presence of the cupric ion bound to the nitrogen atom of CN^- weakens the crystal field strength of CN^- at the ferric ion, presumably shifting the energy of the hole in d_{yz} and causing the near-IR CT band to move. This example draws attention to potentially subtle effects on the crystal field strength at the ferric ion caused by the protein. H bonding of an axial ligand to change the crystal field strength is one obvious way in which a ligand might acquire an unexpected position in the assignment sequence.

The spectroscopic methods discussed here are sensitive to these effects. Hence, they can never be applied by rote. Judicious use allied with knowledge from other techniques, and where possible from sequence data, is needed in order to reach a definitive conclusion.

Acknowledgment. Thanks are due to the SERC and the Royal Society who have provided grants for both equipment and personnel to support this work. We are indebted to the many biochemists who have generously supplied us with protein samples. Their names can be found in the reference list.

(41) Sorrell, T. N.; Martin, P. K.; Bowden, E. F. *J. Am. Chem. Soc.* **1989**, *111*, 766–767.

(42) Gadsby, P. M. A.; Hartshorn, R. T.; Moura, J. J. G.; Sinclair-Day, J. D.; Sykes, A. G.; Thomson, A. J. *Biochim. Biophys. Acta* **1989**, *994*, 37–46.

(43) Hill, B. C.; Brittain, T.; Eglinton, D. G.; Gadsby, P. M. A.; Greenwood, C.; Nicholls, P.; Peterson, J.; Thomson, A. J.; Woon, T. C. *Biochem. J.* **1983**, *215*, 57–66.

(44) Godfrey, C.; Coddington, A.; Greenwood, C.; Thomson, A. J. *Biochem. J.* **1987**, *243*, 225–233.

(45) Thomson, A. H.; Gadsby, P. M. A. *J. Chem. Soc., Dalton Trans.*, in press.

(46) **Note Added in Proof**: It has been shown that the protoheme IX group in bacterioferritin is liganded by two methionine residues, leading to a CT band at 2270 nm ($E_{CT} = 4400\ cm^{-1}$). This is the longest wavelength yet recorded for the ferric-to-porphyrin CT band. The energy of this band is predicted by the additivity rule deduced in this work: Cheesman, M.; Thomson, A. J.; Greenwood, C.; Moore, G. R.; Kadir, F. *Nature*, submitted for publication.